PRODUCTION OF ^{232,233}Pa IN ^{6}Li+^{232}Th COLLISIONS IN THE CLASSICAL TRAJECTORY APPROACH

V.P. Aleshin

Institute for Nuclear Research, Kiev, Ukraine

(Received July 23, 1999)

The semiclassical model of nuclear reactions with loosely bound projectiles (V.P. Aleshin, B.I. Sidorenko, *Acta Phys. Pol.* **B29**, 325 (1998)) is refined and compared with experimental data of Rama Rao *et al.* on the excitation function for the production of ^{232,233}Pa in ^{6}Li+^{232}Th collisions at E = 30–50 MeV. The main contribution to the production of ^{232}Pa is the 2 neutron emission from excited states of ^{234}Pa formed in the (^{6}Li,α) reaction. The main source of ^{233}Pa is the (^{6}Li,αp) reaction followed by γ transitions from excited states of ^{233}Th to ^{233}Th (g.s.) which transforms to ^{233}Pa through β^- decay. The ground state of ^{6}Li regarded as a combination of $n+p+\alpha$ is modeled with the $K=2$, $\boldsymbol{l}_x=\boldsymbol{l}_y=0$ hyperspherical function. The calculation underpredicts the excitation function of ^{232}Pa by a factor of 0.6 and overpredicts the excitation function of ^{233}Pa by a factor of 2.3, on the average. With the more realistic wave function of ^{6}Li both factors are expected to be closer to 1.

PACS numbers: 24.10.–i, 24.10.Lx, 25.60.–t

1. Introduction

In [1] we formulated the semiclassical model of low energy reactions induced by projectiles which are loosely bound towards decay in two or three particles. The reactions were assumed to proceed as dissociation of the projectile into its constituent particles, each of which may later be absorbed by the target or bypass it. The model develops the ideas of classical description of direct reactions followed by fission [2–4] and extends the semiclassical theory of Coulomb excitation [5,6] to the transitions to the unbound states.

Having applied the model to the d+^{93}Nb collisions at E = 15–25 MeV we found [1], that the total cross sections of (d,p), (d,n) and complete fusion reactions reasonably agree with quantum results [7] and experimental data [8]. To illustrate the model for projectiles composed of three particles, the integrated cross sections were calculated for ^{6}He $(=\alpha+n+n)$ induced reactions following collisions with ^{232}Th at few MeV above the Coulomb barrier.

For three-particle projectiles it is impossible to test the semiclassical model by comparison with quantum calculations because the latter are limited to the case of 2-body projectiles [9]. Alternatively the model could be verified by comparing the predicted cross sections of ^{6}He induced reactions with experimental data. However experimental data on energy-integrated cross sections of ^{6}He induced reactions on heavy targets at energies near to and below the Coulomb barrier are very scarce.

Most experiments with such beams are limited to elastic scattering (*e.g.* see [10–12]) and reactions on *light* nuclei in which cases our model is not valid. Experimental cross sections on fission and fusion reactions in the system of ^{6}He+^{209}Bi near the Coulomb barrier were reported in [13] and [14], respectively. Since these are the very first measurements their use to check a new model would not be conclusive.

Therefore we decided to verify the model by analysing experimental data with ^{6}Li beams taking into consideration that these are far less exotic than those of ^{6}He while the wave function of ^{6}Li regarded as a system consisting of $n + p + \alpha$ is similar to that of ^{6}He [15].

As a test case we take the excitation functions of ^{6}Li induced reactions on ^{232}Th leading to the radioactive residual nuclei ^{233,232}Pa in the range of the bombarding energy E = 28–48 MeV measured using the activation of stacked foils technique [16]. The results presented in [16] somewhat disagree with the pioneer experiment [17] based on a different technique.

2. Wave function of ^{6}Li

For a recent review of the models of six-nucleon systems see [18]. According to [15], the ground state wave functions of ^{6}He and ^{6}Li look similarly to each other although their spins differ (1^{+} in ^{6}Li *vs* 0^{+} in ^{6}He). Therefore, in the present work, the wave function of ^{6}Li in the configuration space was taken the same as that of ^{6}He. The spin-isospin factor of the wave function is not needed in our semiclassical model.

According to Filippov *et al.* [19], the hyperradial potential in ^{6}He is

$$V(\rho) = -\frac{V_0}{1 + (\rho/a)^3}, \quad V_0 = 87\,\mathrm{MeV}, \quad a = 3.073\,\mathrm{fm}. \tag{1}$$

We used the same formfactor for the potential in ^{6}Li, having adjusted only V_0 in order to ensure the correct binding energy of ^{6}Li, $B(^{6}\mathrm{Li})$ = 3.7 MeV, rather than 0.96 MeV in ^{6}He.

In the first order of the perturbation theory the hyperradial wave function $\chi(\rho)$ does not change while

$$V_0(^6\mathrm{Li}) = V_0(^6\mathrm{He}) + \left(B(^6\mathrm{Li}) - B(^6\mathrm{He})\right)\left[\int_0^\infty \chi^2(\rho)\frac{d\rho}{1+(\rho/a)^3}\right]^{-1}. \quad (2)$$

Since the relative difference between $V_0(^6\mathrm{Li}) = 97$ MeV found from Eq. (2) and $V_0(^6\mathrm{He}) = 87$ MeV is small, the perturbation theory is validated.

Numerical values of $\chi(\rho)$ were taken from [19]. As angular part of the wave function of ^{6}Li in the 6-dimensional space we used the hyperspherical harmonic with $K = 2$, $\boldsymbol{l}_x = \boldsymbol{l}_y = 0$. Then the distribution probability over $\boldsymbol{x}, \boldsymbol{y}$ is given by

$$|\Psi(\boldsymbol{x},\boldsymbol{y})|^2\, d\boldsymbol{x} d\boldsymbol{y} \sim \chi^2(\rho)\sin^2 4\theta\, d\theta\, d\rho\, d\hat{\boldsymbol{x}}\, d\hat{\boldsymbol{y}}, \quad (3)$$

where

$$\boldsymbol{x} = \frac{1}{\sqrt{2}}(\boldsymbol{r}_p - \boldsymbol{r}_n), \quad \boldsymbol{y} = \frac{2}{\sqrt{3}}\left(\boldsymbol{r}_\alpha - \frac{\boldsymbol{r}_p + \boldsymbol{r}_n}{2}\right), \quad (4)$$

$\boldsymbol{r}_\alpha$, $\boldsymbol{r}_p$, $\boldsymbol{r}_n$ are the positions of α, p, n. On the right hand side of Eq. (3) we have restored $d\rho$ which has been missed in [1]. Taking into account that

$$\rho = \sqrt{x^2+y^2}, \qquad \tan\theta = x/y\,, \quad (5)$$

we find

$$d\theta d\rho = \frac{dx dy}{\sqrt{x^2+y^2}}. \quad (6)$$

Combining this relation with (3) we obtain the distribution over x, y :

$$p(x,y) = \int |\Psi(\boldsymbol{x},\boldsymbol{y})|^2\, d\hat{\boldsymbol{x}} d\hat{\boldsymbol{y}} \sim \frac{\chi^2\left(\sqrt{x^2+y^2}\right)}{\sqrt{x^2+y^2}}\frac{x^2y^2(y^2-x^2)^2}{(x^2+y^2)^4}. \quad (7)$$

This function is plotted in Fig. 1.

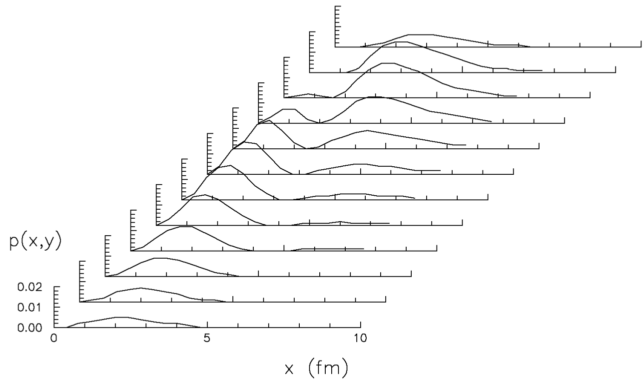

Fig. 1. Probability distribution $p(x,y)$ for the wave function of Eq. (3). From top to bottom y increases from 0.5 fm to 6 fm by 0.5 fm step. The dinucleon and cigarlike configurations are determined as those for which $x < y$ and $x > y$, respectively.

3. Trajectory calculations

The distribution function (3) was used to generate randomly $\boldsymbol{x}$, $\boldsymbol{y}$ which then were used to specify the initial positions of n, p, α in the center of mass system of ^{6}Li. As described in [1], given $\boldsymbol{x}$, $\boldsymbol{y}$ one can find the initial momenta of n, p, and α particle from the expressions involving the binding energy of ^{6}Li, its K value and hyperradial potential.

Given initial positions and momenta of n, p, α inside ^{6}Li which is about to move towards the target with energy E and angular momentum L, we find $\boldsymbol{r}_\alpha$, $\boldsymbol{r}_p$, $\boldsymbol{r}_n$ and particle momenta in the absolute system and put these quantities into Hamilton's equations for $\nu = n, p, \alpha$. Along with $V(\rho)$ these equations include the real parts $U_\nu(r)$ of particle-nucleus optical potentials, $U_\nu(r) + iW_\nu(r)$.

The solutions of Hamilton's equations (found with the RKFS code [20]) together with the imaginary parts $W_\nu(r)$ were used to find for each trajectory s the appropriate survival and absorption factors

$$P_\nu^{(s)} = \exp\left[\frac{2}{\hbar}\int\limits_0^{t_f} dt\Theta\left(\varepsilon_\nu^{(s)}(t)\right) W_\nu(r_\nu^{(s)}(t))\right],\ Q_\nu^{(s)} = 1 - P_\nu^{(s)}\,, \qquad (8)$$

where $t_f \to \infty$. The step function $\Theta(\varepsilon)$ is equal to 1 for positive intrinsic current energies of ^{6}Li and zero otherwise.

The excitation energies of recoil nuclei are denoted by E_x. For instance, in the reactions ($^6\mathrm{Li}, \alpha p$), ($^6\mathrm{Li}, \alpha n$) and ($^6\mathrm{Li}, \alpha$), these are given by

$$E_x^{(s)}(^{233}\mathrm{Th}) \;=\; K_n^{(s)} + U_n^{(s)} - B(^{232}\mathrm{Th}) + B(^{233}\mathrm{Th}),$$

$$
\begin{aligned}
E_x^{(s)}(^{233}\mathrm{Pa}) &= K_p^{(s)} + U_p^{(s)} - B(^{232}\mathrm{Th}) + B(^{233}\mathrm{Pa}), \\
E_x^{(s)}(^{234}\mathrm{Pa}) &= K_n^{(s)} + U_n^{(s)} + K_p^{(s)} + U_p^{(s)} - B(^{232}\mathrm{Th}) + B(^{234}\mathrm{Pa}), \quad (9)
\end{aligned}
$$

where $K_n^{(s)}$, $K_p^{(s)}$, $U_n^{(s)}, U_p^{(s)}$ are the kinetic energies and potentials of n and p in the field of ^{232}Th at $t = t_f$ and B is the binding energy of a nucleus indicated in parentheses [21].

This information was used to construct the partial reaction probabilities $T_c(L, E_x)$, where c denotes the type of the reaction. For the reactions (^{6}Li$, \alpha p$), (^{6}Li$, \alpha n$) and (^{6}Li$, \alpha$) we have:

$$
\begin{aligned}
T_{\alpha p}(L, E_x) &= \frac{1}{N} \sum_{s=1}^{N} \mathcal{P}(\varepsilon_f^{(s)}; E_x - E_x^{(s)}) P_\alpha^{(s)} P_p^{(s)} Q_n^{(s)}, \\
T_{\alpha n}(L, E_x) &= \frac{1}{N} \sum_{s=1}^{N} \mathcal{P}(\varepsilon_f^{(s)}; E_x - E_x^{(s)}) P_\alpha^{(s)} Q_p^{(s)} P_n^{(s)}, \\
T_{\alpha}(L, E_x) &= \frac{1}{N} \sum_{s=1}^{N} \mathcal{P}(\varepsilon_f^{(s)}; E_x - E_x^{(s)}) P_\alpha^{(s)} Q_p^{(s)} Q_n^{(s)}. \quad (10)
\end{aligned}
$$

The factor $\mathcal{P}(\varepsilon; \Delta)$ is equal to 1 if $\varepsilon > 0$ and $|\Delta| <$1 MeV and zero otherwise; $\varepsilon_f^{(s)}$ is the intrinsic energy of the $\alpha + n + p$ system at $t = t_f$, N is the total number of samples at given L. Equations (10) are equivalent to the procedure of Ref. [1] if 'recombination' of n, p, α back to ^{6}Li is negligible.

The cross sections are given by

$$
\sigma_c(E_x) = \frac{\pi \hbar^2}{2ME} \sum_L (2L+1) T_c(L, E_x), \quad (11)
$$

where M is the mass of the projectile. It is assumed that M is much smaller than the target mass. Please note that a factor of 2 should be dropped in the expression for σ_c on p. 328 of Ref. [1].

In the following calculations, the parameters of the optical potentials for n, p, α are taken from [22, 23] and $N = 200$.

4. Production of ^{232,233}Pa at $E(^6\mathrm{Li}) = 40$ MeV

In Fig. 2, we show the cross sections

$$
\sigma(^6\mathrm{Li}, \alpha p; E_x), \quad \sigma(^6\mathrm{Li}, \alpha n; E_x), \quad \text{and} \quad \sigma(^6\mathrm{Li}, \alpha; E_x) \quad (12)
$$

for the production of ^{233}Th, ^{233}Pa, and ^{234}Pa, respectively, by the ^{6}Li beam of $E = 40$ MeV on the ^{232}Th target as functions of the excitation energy E_x of the appropriate recoil nucleus.

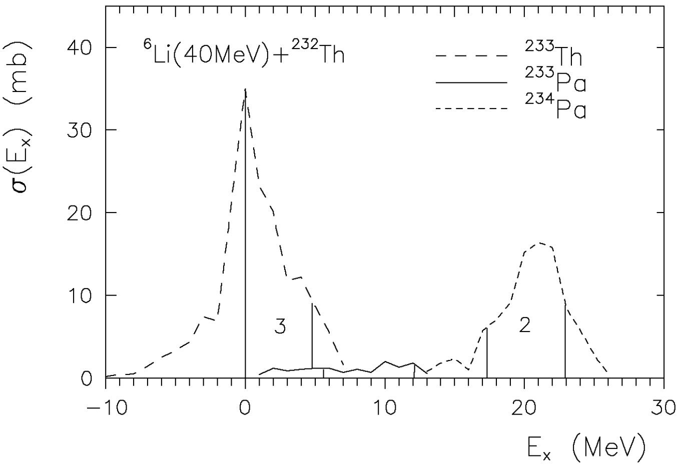

Fig. 2. Excitation energy distributions of ^{233}Th and ^{233,234}Pa produced in the ^{6}(Li,αp), ^{6}(Li,αn) and ^{6}(Li,α) reactions on ^{232}Th at the beam energy of 40 MeV. The vertical lines are drawn at $E_x = S_n(^{233}\mathrm{Th})$, $S_n(^{233}\mathrm{Pa})$, $S_n(^{233}\mathrm{Pa}) + S_n(^{232}\mathrm{Pa})$, $E_{x0} - \frac{1}{2}S_n(^{232}\mathrm{Pa})$, and $E_{x0} + \frac{1}{2}S_n(^{232}\mathrm{Pa})$ (from left to right). Marked by '2' and '3' are the areas contributing to the production of ground state nuclei of ^{232}Pa and ^{233}Pa, respectively.

One can see that some part of ^{233}Th nuclei is formed at negative E_x. This occurs when neutrons are getting captured to the single-particle states lying below the Fermi energy. After exclusion of such events forbidden by the Pauli principle all cross sections will increase by a factor of $N/(N - N_<)$, where $N_<$ is the number of recoil nuclei with $E_x < 0$.

The cross section for the production of ^{233}Pa is very small compared to the production cross sections of ^{233}Th and ^{234}Pa. This simply reflects the small probability of the events in which proton is captured whereas neutron avoids absorption compared to the probability for absorption of either n or n and p. In the following the contribution to the production of ^{232,233}Pa(g.s.) from de-excitation of ^{233}Pa is neglected.

As shown in Fig. 2, the major source of production of ^{233}Pa(g.s.) is a region marked by '3' which extends from $E_x = 0$ up to the neutron emission threshold $S_n(^{233}\mathrm{Th})$=4.79 MeV. The states in this region de-excite by γ -emission to the ground state of ^{233}Th which in its turn is converting into ^{233}Pa through β^- decay.

The main source of production of ^{232}Pa(g.s.), marked by '2', is the 2-neutron decay of ^{234}Pa to the states of ^{232}Pa with $E_x < S_n(^{232}\mathrm{Pa})$=5.6 MeV. The contribution of this source is estimated as

$$\sigma_2(^{232}\mathrm{Pa}) \approx R_\mathrm{n}(E_{x1})R_\mathrm{n}(E_{x0}) \int\limits_{E_{x0}-\frac{1}{2}S_n(^{232}\mathrm{Pa})}^{E_{x0}+\frac{1}{2}S_n(^{232}\mathrm{Pa})} dE_x\sigma(^6\mathrm{Li},\alpha;E_x), \qquad (13)$$

where E_{x0}, E_{x1} are the mean excitation energies before and after emission of the first neutron; $R_\mathrm{n}(E_{x0})$ and $R_\mathrm{n}(E_{x1})$ are the branching ratios for neutron emission from ^{234}Pa at $E_x = E_{x0}$ and ^{233}Pa at $E_x = E_{x1}$, respectively.

Treating the emission of the first and the second neutrons in the framework of preequilibrium and equilibrium models, respectively, allows one to express E_{x1} in terms of $S_n(^{232}\mathrm{Pa})$ and $S_n(^{233}\mathrm{Pa})$ and present E_{x0} through E_{x1}, $S_n(^{234}\mathrm{Pa}) = 5.2$ MeV and the exciton number n_0 in the initial configuration of ^{234}Pa (for details see Appendix).

The neutron branching ratio is given by

$$R_\mathrm{n} = \frac{1/\tau_\mathrm{n}}{1/\tau_\mathrm{n} + 1/\tau_\mathrm{f}}, \qquad (14)$$

where τ_n is the nuclear decay time via the neutron channel and τ_f is the fission lifetime. Taking these times from [24] we find that $R_\mathrm{n}(E_x)$ in ^{233}Pa linearly increases from 0.6 to 0.7 when E_x increases from 7 to 12 MeV. From Eq. (17) in the Appendix we estimated that $E_{x1} = 10$ MeV which gives $R_\mathrm{n}(E_{x1}) = 0.66$.

From Eq. (20) in the Appendix we found that $E_{x0} = 20.1$ and 18.4 MeV at $n_0 = 4$ and 5, respectively, and we put $R_\mathrm{n}(E_{x0}) = 1$. A linear extrapolation of the neutron branching ratio to $E_x \approx 20$ MeV would give 0.85. However, the pre-equilibrium (fast) mechanism of neutron emission is expected to prevail at this excitation energy to make the branching ratio close to 1.

5. Discussion and conclusion

The type of trajectory calculations illustrated in Fig. 2 were repeated for few values of ^{6}Li beam energy in the range of 30–50 MeV with a 5 MeV step. They are summarized in a form of excitation functions for the production of ^{232,233}Pa in ^{6}Li+^{232}Th collisions which are presented in Fig. 3 together with experimental points [16].

Looking at Fig. 3 one can see that there is as much general agreement as might be anticipated accounting for a simplistic wave function of ^{6}Li, employment of the hyperradial and mean field potential concepts and using

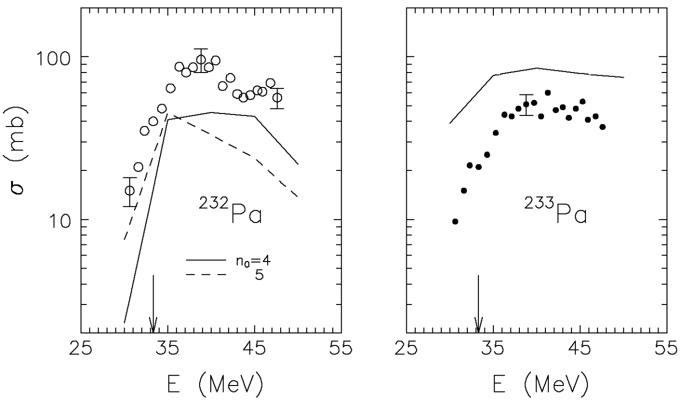

Fig. 3. Excitation functions for the production of ^{232}Pa (left) and ^{233}Pa (right) in ^{6}Li+^{232}Th collisions at E = 30–50 MeV. The arrows indicate the position of the Coulomb barrier.

quite schematic picture of the de-excitation stage. On the average, the excitation function of ^{232}Pa is underpredicted by a factor of 0.6 while the excitation function of ^{233}Pa is overpredicted by a factor of 2.3.

As seen from Fig. 3, the choice $n_0 = 5$ is preferable at low beam energies while at high energies $n_0 = 4$ reproduces the data better. This is probably connected to the fact that the contribution of direct mechanism increases with the growing energy of the beam, hence of the excitation energy of the recoil nucleus of ^{234}Pa.

Using Eq. (7) for the $p(x, y)$ distribution in ^{6}Li one can show that dinucleon and cigarlike configurations (which can be separated by the line $y = x$ in Fig. 1) have equal weights. More realistic wave functions [15] give rise to higher probability for dinucleon than for cigar: 73% *vs* 27% and 76% *vs* 24% in ^{6}He [25] and ^{6}Li [26], respectively.

With the enhancement of the dinucleon configuration the yield of ^{234}Pa originating from the capture of correlated p-n pairs is expected to increase. Accordingly, the production of ^{232}Pa increases too. The cigarlike configuration contributes to the events when neutron is captured while proton avoids absorption. Therefore with the suppression of this configuration the yield of ^{233}Th, hence of ^{233}Pa, should decrease. Thus, the improved wave function of ^{6}Li is expected to drive the yields of both ^{232}Pa and ^{233}Pa towards better agreement with the data.

I am grateful to Prof. N.G. Nicolis for the discussions which initialized our work on reactions with loosely bound projectiles. Valuable comments on the preliminary versions of the paper were made by Profs. G.F. Filippov, I.N. Vishnevsky, I.A. Korzh, V.A. Plujko, Yu.V. Kibkalo and N.I. Zaika. Dr. A.I. Sanzhur kindly provided us with his version of RKFS code. Mrs. O.M. Kuprava of Information Department helped with searching of data.

Appendix

The mean excitation energy of ^{232}Pa below the neutron emission threshold is given by

$$E_{x2} = \frac{1}{2} S_n(^{232}\mathrm{Pa})\,, \tag{15}$$

while the corresponding temperature is

$$T_2 = \sqrt{\frac{E_{x2}}{a_2}},\ a_2 = 232/8\,. \tag{16}$$

By definition, the mean excitation energy E_{x1} of ^{233}Pa is shifted with respect to E_{x2} by the mean energy carried away by a neutron evaporated from ^{233}Pa:

$$E_{x1} = E_{x2} + 2T_2 + S_n(^{233}\mathrm{Pa})\,. \tag{17}$$

The mean excitation energy E_{x0} of ^{234}Pa is shifted with respect to E_{x1} by the mean energy carried away by a neutron emitted from ^{234}Pa. Given initial exciton number n_0, the pre-equilibrium energy spectrum is given by [27, 28]

$$N(\epsilon)d\epsilon \sim \epsilon\sigma_{\mathrm{inv}}(\epsilon)(E_{x0} - S_n - \epsilon)^{n_0-2} d\epsilon\,. \tag{18}$$

Let $\epsilon_{\max}$ be the value of ϵ where $N(\epsilon)$ attains maximum. Treating $\sigma_{\mathrm{inv}}(\epsilon)$ as a constant near $\epsilon = \epsilon_{\max}$ we find

$$\epsilon_{\max} = \frac{E_{x0} - S_n}{n_0 - 1}\,. \tag{19}$$

Replacing the mean neutron kinetic energy with $\epsilon_{\max}$ we obtain:

$$E_{x0} = E_{x1} + S_n(^{234}\mathrm{Pa}) + \frac{E_{x0} - S_n(^{234}\mathrm{Pa})}{n_0 - 1} \tag{20}$$

which yields

$$E_{x0} = \frac{n_0 - 1}{n_0 - 2} E_{x1} + S_n(^{234}\mathrm{Pa}). \tag{21}$$

REFERENCES

[1] V.P. Aleshin, B.I. Sidorenko, *Acta Phys. Pol.* **B29**, 325 (1998).

[2] V.M. Strutinsky, *Yad. Fiz.* **1**, 588 (1965).

[3] K.L. Wolf, R. Vandenbosch, W.D. Loveland, *Phys. Rev.* **170**, 1059 (1968).

[4] V.P. Aleshin, *Yad. Fiz.* **36**, 48 (1982).

[5] K. Alder, A. Winther, *Electromagnetic Excitations*, North Holland, Amsterdam 1975.

[6] V.P. Aleshin, S.R. Ofengenden, *Izv. Akad. Nauk SSSR, Ser. Fiz.* **44**, 1075 (1980); *Bull. Acad. Sci. USSR, Phys. Ser.* **44**, no. 5, 154 (1980).

[7] R.C. Mastroleo, T. Udagawa, M.G. Mustafa, *Phys. Rev.* **C42**, 683 (1990).

[8] J. Pampus, J. Bisplinghoff, J. Ernst, T. Mayer-Kuckuk, J. Rama Rao, G. Baur, F. Roesel, D. Trautmann, *Nucl. Phys.* **A311**, 141 (1978); J. Kleinfeller, J. Bisplinghoff, J. Ernst, T. Mayer-Kuckuk, G. Baur, B. Hoffmann, R. Shyam, F. Roesel, D. Trautmann, *Nucl. Phys.* **A370**, 205 (1981).

[9] M.G. Mustafa. Projectile Breakup Hauser–Feshbach Modeling, in: G. Reffo, A. Ventura, C. Grandi (Eds) "Nuclear Data for Science and Technology", Conference Proceedings, vol. 59, part 1, SIF, Bologna 1997, p. 274.

[10] R.J. Smith, J.J. Kolata, K. Lamkin, A. Morsad, K. Ashktorab, F.D. Becchetti, J.A. Brown, J. W. Jänecke, W.Z. Liu, D.A. Roberts, *Phys. Rev.* **C43**, 761 (1991).

[11] R.E. Warner, F.D. Becchetti, J.W. Jänecke, D.A. Roberta, D. Butts, C.L. Carpenter, J.M. Fetter, A.Muthukrishnan, J.J. Kolata, K. Lamkin, M. Belbot, M. Zahar, A. Galonsky, K. Ieki, P. Zecher, *Phys. Rev.* **C51**, 178 (1995).

[12] V.P. Verbitsky, V.A. Kiva, A.A. Klipenstein, O.F. Nemets, Yu.N. Pavlenko, K.O. Terenetsky, Th. Delbar, J. Vervier, K. Marche, E. Lienard, P. Leleux, *Ukr. Fiz. Zh.* **43**, no. 3, 268 (1998).

[13] Yu.E. Penionzhkevich, E.A. Cherepanov, I. David, A.S. Fomichev, R. Kalpakchieva, S.M. Lukyanov, Yu.Ts. Oganessian, N.K. Skobelev, O.B. Tarasov, R. Wolski, Z. Dlouhy, *Nucl. Phys.* **A583**, 791c (1995); Yu. E. Penionzhkevich, *Nucl. Phys.* **A588**, 259c (1995).

[14] J.J. Kolata, V. Guimarães, D. Peterson, P. Santi, R. White-Stevens, P.A. DeYoung, G. F. Peasly, B. Hughey, B. Atalla, M. Kern, P.L. Jolivette, J.A. Zimmerman, M.Y. Lee, F.D. Becchetti, E.F. Aguilera, E. Martinez-Quiroz, J.D. Hinnefeld, *Phys. Rev. Lett.* **91**, 4580 (1998).

[15] B.V. Danilin, M.V. Zhukov, S.N. Ershov, F.A. Gareev, R.S. Kurmanov, J.S. Vaagen, J.M. Bang, *Phys. Rev.* **C43**, 2835 (1991).

[16] J. Rama Rao, J. Ernst, H. Machner, *Nucl. Phys.* **A448**, 365 (1986).

[17] A. Fleury, G.N. Simonoff, *Phys. Lett.* **14**, 44 (1965).

[18] V.S. Vasilevsky, A.V. Nesterov, F. Arickx, P. van Leuven, *Yad. Fiz.* **60**, 413 (1997).

[19] G.F. Filippov, I.Yu. Rybkin, S.V. Korennov, *Yad. Phys.* **59**, 616 (1996).

[20] G.E. Forsythe, M.A. Malcolm, C.B. Moler, Computer Methods for Mathematical Computations, Prentice Hall, Englewood Cliffs, NJ, 1977.

[21] A.H. Wapstra, K. Bos, *Atomic Data and Nuclear Data Tables* **19**, 175 (1977).

[22] P.E. Hodgson, *Nuclear Reaction and Nuclear Structure*, Clarendon Press, Oxford 1971, p. 178.

[23] N.I. Zaika, Yu.V. Kibkalo, O.F. Nemets, V.S. Semenov, V.P. Tokarev, P.L. Shmarin, *Izv. Akad. Nauk SSSR Ser. Fiz.* **40**, 1294 (1976).

[24] D.O. Eremenko, V.O. Kordyukevich, S.Yu. Platonov, O. V. Fotina, O.A. Yuminov, G. Giardina, F. Malaguti, G. Vannini, *Nucl. Phys.* **A589**, 395 (1995).

[25] Yu.Ts. Oganessian, V.I. Zagrebaev, J.S. Vaagen, in: International Conference on Nuclear Physics "Nuclear Shells–50 Years", XLIX Meeting on Nuclear Spectroscopy and Nuclear Structure, April 21–24, 1999, Dubna, Russia, St. Petersburg 1999, p. 275.

[26] V.I. Zagrebaev, private communication.

[27] K. Seidel, D. Seeliger, R. Reif, V. D. Toneev, *Physics of Elementary Particles and Atomic Nuclei* 7, part 2 (1976) 499, p. 517.

[28] C.K. Cline, M. Blann, *Nucl. Phys.* **A172**, 225 (1971).